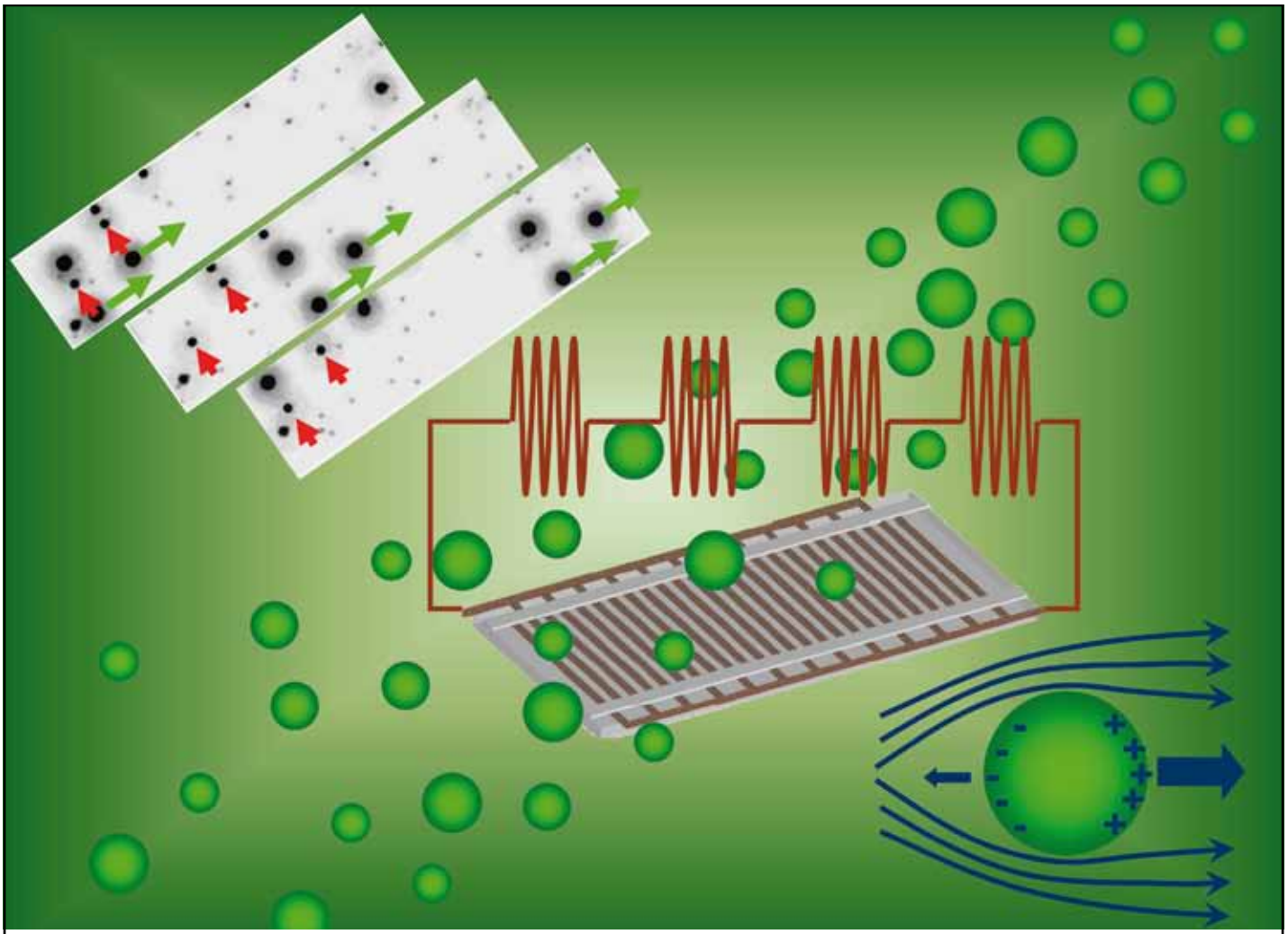

Featuring research from Computational Engineering Programme of Singapore-MIT Alliance.

Title: Separation of particles by pulsed dielectrophoresis.

A tunable particle-sorter for microfluidic applications using time-modulated dielectrophoresis. By pulsing the dielectrophoretic force in time, the order of separation of particles by size can be changed and mid-size particles can be extracted from a heterogeneous population in one step.

As featured in:

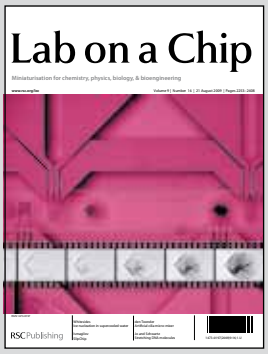

See Lim *et al.*, *Lab Chip*, 2009, **9**, 2306–2312.

RSC Publishing

www.rsc.org

Registered Charity Number 207890

Separation of particles by pulsed dielectrophoresis†

Hai-Hang Cui,[a] Joel Voldman,[cd] Xue-Fei He[a] and Kian-Meng Lim*[ab]

Received 30th March 2009, Accepted 9th June 2009
First published as an Advance Article on the web 29th June 2009
DOI: 10.1039/b906202e

In this paper, we introduce a dielectrophoresis (DEP)-based separation method that allows for tunable multiplex separation of particles. In traditional DEP separations where the field is applied continuously, size-based separation of particles uses the cubic dependence of the DEP force on particle radius, causing large particles to be retained while small particles are released. Here we show that by pulsing the DEP force in time, we are able to reverse the order of separation (eluting the large particles while retaining the small ones), and even extract mid-size particles from a heterogeneous population in one step. The operation is reminiscent of prior dielectrophoretic ratchets which made use of DEP and Brownian motion, but we have applied the asymmetric forces in time rather than in a spatial arrangement of electrodes, thus simplifying the system. We present an analytical model to study the dynamic behavior of particles under pulsed DEP and to understand the different modes of separation. Results from the model and the experimental observations are shown to be in agreement.

Introduction

Microscale separation technologies are increasing in importance in many research fields across biology and chemistry. Separation technologies aim to extract targets, such as cells and biomolecules, at high purity, in order to be useful for monitoring, screening, detection and amplification. One recent trend in microfluidic separations has been to develop more flexible and controllable separation methods that allow spatial separation of multi-component mixtures.[1–4]

Dielectrophoresis (DEP) is one common separation technique, which acts on polarizable particles suspended in fluids.[5–8] DEP provides us with several parameters, such as voltage, phase and frequency of the AC current used, to control the separation process. By varying these parameters, it is possible to separate particles with different polarizabilities. The DEP force may be used in conjunction with other forces, most notably hydrodynamic forces, and the interaction among these forces can result in the desired separation process. Most existing DEP-based separation methods are based on application of the DEP force continuously in time, such as DEP field-flow fractionation (DEP-FFF),[9] iso-dielectric separation,[10] and lateral dielectrophoresis.[11–13]

Besides a continuous-time force field, discontinuous or time-varying force fields may be used for particle separation in microfluidics.[14–18] The thermal/Brownian ratchet is a DEP-based technique that uses a time-varying external force.[3,16–18] In ratcheting separations, particles are first trapped by an attractive DEP force generated by an asymmetrical electrode structure and then released by turning off the electric field. The particles will then diffuse isotropically from the collection point until some of them fall into the capture zone of the next pair of electrodes along the ratchet. Net particle motion is produced by repeating the process of capture and release over time. The mobility of the particles depends on the particle size, allowing the particles to be separated by size after many cycles. Brownian ratchets require particle diffusion to be significant in order to enact separations, and as such are only suitable for very small particles.

In our present work, we introduce a discontinuous (in time) force into a microfluidic system for particle separation. Pulsed DEP is used to provide the oscillatory force, and we can control the parameters of the pulsed DEP to tune its interaction with existing fluid forces in the fluid channel. In this fashion we can sort out particles of specific sizes in a heterogeneous population and, specifically, we can sort out intermediate-sized particles from larger and smaller particles. The method works by first turning on a negative DEP force to block all particles at the upstream region of electrode; then the DEP force is switched off for a short period to release the particles downstream. Since the fluid forces acting on particles of different sizes vary, the particles will attain different velocities and end up at different locations after a period of time. Some of them will have moved past the electrode, while others will not. By turning the DEP force on again after a specific period of time, the particles not yet past the electrode will be pushed back upstream while the others will be flushed downstream. By tuning the time period and relative strength of the DEP force, we can select specific sizes of particles to be released downstream from a heterogeneous mixture. We present an analytical model to illustrate the dynamics of this method along with experimental results demonstrating separation of 3, 5 and 10 μm polystyrene beads. The setup of the microdevice is illustrated in Fig. 1.

Modeling and results

Balance of DEP and drag forces in pulsed-DEP

The typical time scale of the moving particle in a microchannel is given by L/U_f, where L is the characteristic length dimension and

[a]*Singapore-MIT Alliance, National University of Singapore, 4 Engineering Drive 3, 117576, Singapore. E-mail: smach@nus.edu.sg*
[b]*Department of Mechanical Engineering, National University of Singapore, 9 Engineering Drive 1, 117576, Singapore. E-mail: limkm@nus.edu.sg*
[c]*Research Laboratory of Electronics, MIT, Cambridge, MA, USA. E-mail: voldman@mit.edu*
[d]*Microsystems Technology Laboratories, MIT, Cambridge, MA, USA*
† Electronic supplementary information (ESI) available: Supplementary figures and ESI movies. See DOI: 10.1039/b906202e

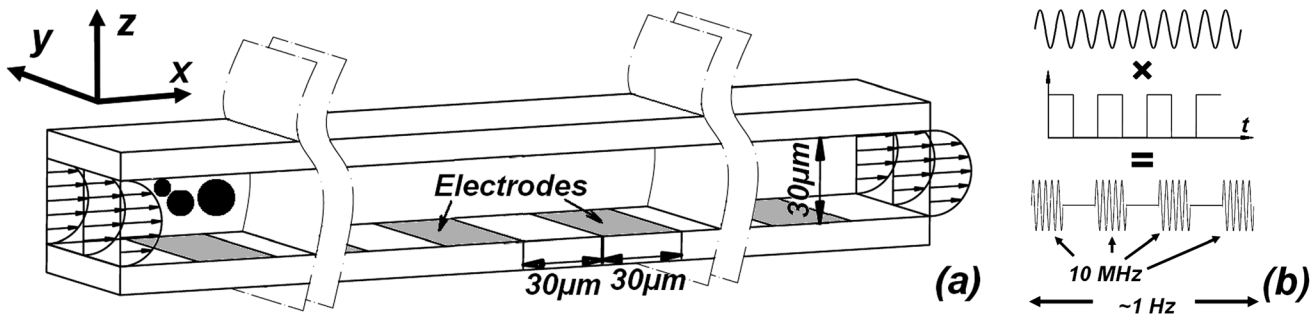

Fig. 1 Schematic of pulsed-DEP device (not to scale). (a) Flow is from left to right. The interdigital electrodes are patterned at the bottom of a microchannel of width 5.65 mm. Beads are levitated by nDEP to the channel ceiling, where the interaction of pulsed nDEP force and fluid flow enacts a separation. Pulsed DEP provides the oscillatory force. (b) Schematic showing how a sine wave is time-multiplexed by a square wave to obtain the pulsed-DEP waveform. The sine wave is typically about 10^7 times higher in frequency than the square wave (not to scale here).

U_f is the local flow velocity. For typical values of L (which is of the order of 10 μm as given by the width of electrode) and U_f (which is of the order of 100 μm/s) in our experimental microchannel, the resulting time scale is about $0.1 \sim 1$ second. When the DEP force is modulated in time at this time scale of fluid/particle motion, we have an additional parameter to control the separation process. In the present design, we pulse the DEP force by turning it on and off with a 50% duty-cycle square wave with frequency <10 Hz. The pulse frequency is comparable to the fluid flow time scale and much lower than the 10 MHz DEP signal.

Pulsed DEP relies on a competition between a time-varying DEP force and a constant fluid drag to effect separation. To understand how these forces compete, we first derive a semi-analytical formulation for the balance between these forces in continuous DEP and then extend that formulation to pulsed DEP, allowing understanding into how experimental parameters (voltage, pulsing frequency, electrode dimensions, and particle properties) lead to particle capture or to release.

The DEP force on a spherical particle (with radius r, relative permittivity ε_p and conductivity σ_p) suspended in a medium (with relative permittivity ε_f and conductivity σ_f) is given by[5,6]

$$\begin{aligned} F_{DEP} &= 2\pi\varepsilon_0\varepsilon_f r^3 \,\mathrm{Re}\left[K^*(\omega)\right]\nabla E_{rms}^2 \\ K^*(\omega) &= \frac{\varepsilon_p^* - \varepsilon_f^*}{\varepsilon_p^* + 2\varepsilon_f^*} \\ \varepsilon_p^* &= \varepsilon_p - j\frac{\sigma_p}{\omega}, and, \varepsilon_f^* = \varepsilon_f - j\frac{\sigma_f}{\omega} \end{aligned} \quad (1)$$

where E_{rms} is the root mean square of electric field strength, ε_0 is the permittivity in vacuum, and ω is the angular frequency of applied electric field. The direction of DEP force depends on the sign of the Clausius–Mossotti (CM) factor given by the real part of $K^*(\omega)$, and it takes on values from −0.5 to 1. The DEP force is classified as positive DEP force (pDEP) when $CM > 0$ and negative DEP force (nDEP) when $CM < 0$. When a particle experiences nDEP, it is repelled from the region of high electric field. In our situation, the particles are much less polarizable than the medium, and thus the CM factor takes on a value of −0.47.

The DEP force near the top surface of the channel (one radius away from the ceiling) is approximately sinusoidal,[19]

$$|E^2| = AV^2\sin\left(\frac{2\pi x}{\lambda}\right) + \left|E_0{}^2\right| \quad (2)$$

where V is the magnitude of the AC voltage applied at the electrodes, A is a constant corresponding to the geometry of the model and the size of the particle (obtained *via* Comsol simulation), λ is the wavelength of the electrode structure, and $|E_0^2|$ is a constant offset. From this expression, the DEP force can be expressed as,

$$F_{DEP} = \frac{4\pi^2\varepsilon_0\varepsilon_f r^3 \,\mathrm{Re}\left[K^*(\omega)\right]AV^2}{\lambda}\cos\left(\frac{2\pi x}{\lambda}\right) \quad (3)$$

The Stokes force acting on a sphere is given by

$$F_{stokes} = -6\pi c_1\mu r(U_p - U_f) \quad (4)$$

where μ is the viscosity of fluid, U_f is the local flow velocity, U_p is the velocity of the particle, and c_1 is a correction factor to account for near-wall effects.[20,21] We used a boundary element model to calculate the Stokes force on spherical beads near a flat wall, and the correction factor c_1 values are found to be 2.07, 1.86 and 1.78 for 10, 5 and 3 μm particles, respectively. The local flow velocity is given by

$$U_f = \frac{6c_2 r(H-r)}{H^3 W}V_{flow} \quad (5)$$

where, H is height of channel, W is width of channel, V_{flow} is volumetric flow rate, and c_2 is a correction factor determined experimentally (see ESI†). This correction factor accounts for the difference between the actual local velocity at the center of the particle and the velocity predicted from the parabolic profile of Poiseuille flow. This difference could be due to distortion of the parabolic profile due to the presence of the particle, or any slight downward drift of the center of the particle from the assumed depth from the top surface. The correction factor c_2 was determined to be 0.71, 0.91 and 1.11 for 10, 5 and 3 μm particles, respectively. As the density of the particles (1.05 g/cm^3) is close to that of water, the buoyancy force is neglected in the present analysis. Given the viscous nature of our experimental system, the particle attains its terminal velocity immediately and acceleration can be neglected.

The fluid drag and DEP forces can then be combined to give

$$F_{Total} = 6\pi c_1\mu r(U_f - U_p) + F_{DEP} \quad (6)$$

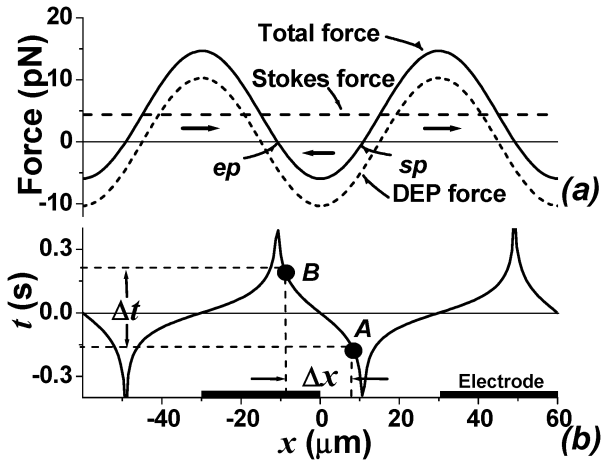

Fig. 2 (a) The plots of the DEP force, Stokes force, and total force on a 5 μm particle at V = 20 Vpp. The force is positive going to the right. Two zero-force points exist: a stable equilibrium point (*ep*) and an unstable separation point (*sp*). (b) A plot of the time evolution of particle position, for the case where $\xi 1 = 50\ \mu m\ s^{-1}$ and $\xi 2 = -117\ \mu m\ s^{-1}$. The time tends to infinity when a particle approaches to equilibrium point and separation point.

This expression can be used to determine stable and unstable holding points (Fig. 2a). The two points where the total force is zero give the two locations where the sphere will come to rest. The left-most location is a stable equilibrium point (*ep*), where a particle from upstream is stopped and cannot move forward, while the right-most location is an unstable equilibrium point, which we denote as the separation point (*sp*). When the particle passes this point (to the right), it will be pushed further away to the right from this point.

To understand the force balance in a time-varying electric field, we first explicitly determine the particle trajectory under the DEP force by integrating the particle velocity. Substituting eqn (3) into eqn (6), the velocity of the particle is then given by

$$U_p = \frac{dx}{dt} = \frac{2\pi\varepsilon_0\varepsilon_f r^2 \mathrm{Re}\left[K^*(\omega)\right] A V^2}{3c_1\mu\lambda}\cos\left(\frac{2\pi x}{\lambda}\right) + U_f \quad (7)$$

Integrating, we get an implicit relation between the position of the particle and time,

$$t(x) = \frac{\lambda}{2\pi}\frac{1}{\sqrt{\xi_2^2-\xi_1^2}}\tanh^{-1}\left(\frac{\sqrt{\xi_2^2-\xi_1^2}\sin\left(\frac{2\pi x}{\lambda}\right)}{\xi_2+\xi_1\cos\left(\frac{2\pi x}{\lambda}\right)}\right) \quad (8)$$

$$\xi_1 = U_f \text{ and } \xi_2 = \frac{2\pi\varepsilon_0\varepsilon_f r^2 \mathrm{Re}\left[K^*(\omega)\right] A V^2}{3c_1\mu\lambda}$$

Here, ξ_2 corresponds to the terminal velocity that a particle can attain in the fluid under the maximum DEP force. For stable particle retention the condition $|\xi_1|<|\xi_2|$ must be satisfied, which implies that the Stokes force is less than the peak DEP force. A plot of time t against the position x is given in bottom panel of Fig. 2 according to eqn (8), for the period when the DEP force is turned on. The figure is interpreted as relating the time taken Δt by a particle to move over a distance travelled Δx. Also, only a positive change in time ($\Delta t > 0$) is possible. Hence, the particle will move from A to B when the DEP force is on, and the motion from B to A is not allowed. For a particle at B, it will have to move (backwards in x) towards the equilibrium point. Also, the time taken to reach the equilibrium point is infinity; this also indicates that a particle will remain at the equilibrium position as long as the DEP force is turned on. A particle placed near to the separation point will readily move away from it for any positive elapsed time Δt, backwards in x for the left branch, or forward in x for the right branch.

Release frequency in pulsed DEP

Combining the particle trajectory under DEP force with the trajectory under drag (derived below), we can determine the conditions under which particles will be retained in pulsed DEP. Starting from the equilibrium point, a particle will drift downstream when the DEP force is turned off. If, during the off period, the particle moves past the separation point, then the particle will be pushed further downstream when the DEP force is turned back on. Hence, for a particle to be retained, there is a maximum allowable time for this off-period and a corresponding lower limit for the pulsing frequency, which we call the release frequency, f_r. An estimate of the maximum allowable time for the off-period, and thus the release frequency, can be obtained from the time taken for the particle to move from the stable equilibrium point to the separation point under Stokes force only,

$$t_{sys} = \frac{x(sp) - x(ep)}{U_f} = \frac{D_{ep-sp}}{U_f} \quad (9)$$

Here, $x(sp)$ and $x(ep)$ represent the coordinates of *ep* and *sp* and $D_{ep\text{-}sp}$ is the distance between the two points.

To determine f_r, we simulate the time evolution of the particle under DEP with a pulsing frequency f. We start the particle at the equilibrium point (*ep*) and calculate the distance travelled by the particle when the DEP is turned off and turned on. When the DEP force is turned off, the particle moves to

$$x_1 = x(ep) + U_f(r)/(2f) \quad (10)$$

When DEP is then turned on for the next half period the position of the particle x_2 can be determined from $t(x_2)-t(x_1) = 1/(2f)$, leading to,

$$x_2 = \left(\sin^{-1}\left(\frac{\xi_2\xi_3}{\sqrt{\xi_2^2-\xi_1^2+\xi_1^2\xi_3^2}}\right) - \alpha\right)\frac{\lambda}{2\pi}$$

$$\xi_3 = \tanh\left(\left(t(x_1)+\tfrac{1}{2f}\right)\tfrac{2\pi}{\lambda}\sqrt{\xi_2^2-\xi_1^2}\right) \quad (11)$$

$$\alpha = \tan^{-1}\left(\frac{-\xi_3\xi_1}{\sqrt{\xi_2^2-\xi_1^2}}\right)$$

Once the DEP force is again turned off, the particle would move to the right, and so on.

Simulating the trajectory over repeated on-off cycles for a given f, we can determine if particle retention occurs (*i.e.*, the final position of the particle after each cycle is stable), and by

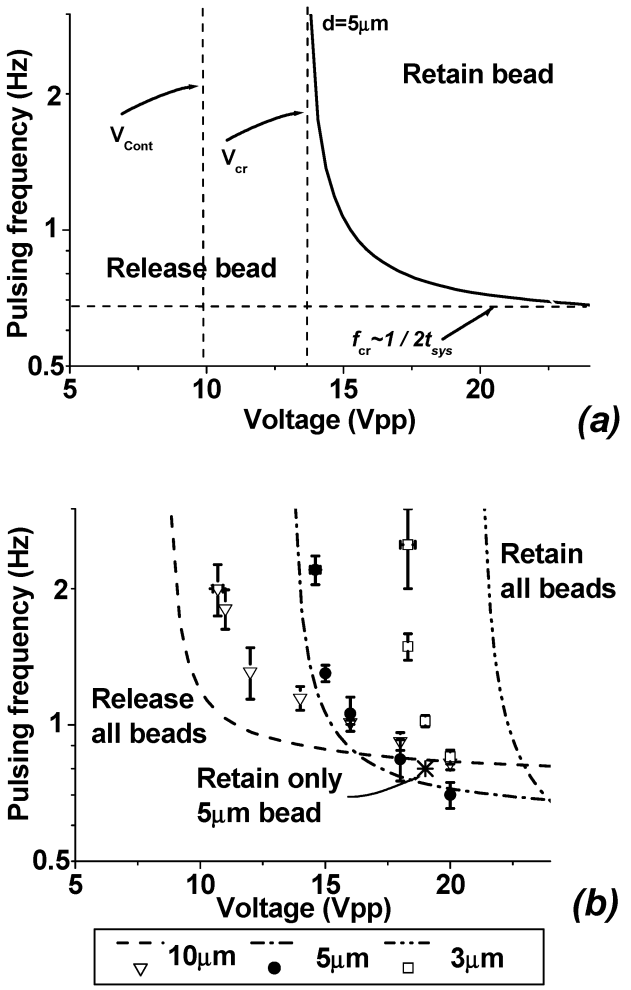

Fig. 3 Release frequency. (a) Plot of the pulsing frequency *f versus* the applied voltage, showing an operating region that retains particles and one that releases particles. There is a minimal voltage (V_{cr}) needed to retain particles while pulsing, which is about 1.4 times the voltage that would be needed without pulsing (V_{cont}). At high voltage the critical frequency approaches a value determined by the time for particles to travel from *ep* to *sp*. (b) Results from the model (shown as lines) and experiments (average shown as points with bar indicating one standard deviation spread for a sample size of 6) for the dynamic behaviour for three particle sizes at a 50 μL/h flowrate. At certain operating conditions, intermediate-sized particles can be retained from large and small particles.

varying *f* we can determine the release frequency f_r. The resulting plots of release frequency *versus* applied voltage show two operating regions: one where particles are retained and one where they are released (Fig. 3a). The line demarcating the two regions has a characteristic shape, bounded at low voltage by a critical voltage, V_{cr}, where f_r increases very sharply. For voltages below this critical voltage, the beads cannot be retained because the nDEP force cannot overcome the hydrodynamic force. This critical voltage is approximately 1.4 times the corresponding release voltage under continous nDEP operation, and has been verified experimentally (see ESI†).

Changing particle size will affect the *f*–*V* characteristic (Fig. 3b). Here we note that there is an operating region (marked by a * in the figure) where only 5 μm beads will be retained but the 3 and 10 μm beads would be released. Hence, if we operate the device at the voltage and pulse frequency within that central region, we should be able to retain mid-size particles (5 μm) among a population of small (3 μm) and large (10 μm) particles.

We performed measurements of f_r *versus* voltage for microparticles of three different sizes (Fig. 3b); consistent with the simulations, as the applied voltage decreases, f_r increases, first gradually, and then sharply below a certain voltage. The f_r characteristics for the 5 μm and 10 μm beads intersect at about 16 V_{pp}, similar to the predicted value. Additionally, f_r for the 10 μm beads is smaller than for the 5 μm beads for $V < 16$ V_{pp}, similar to predictions.

We then used our model to more clearly illustrate why pulsed DEP can separate intermediate-sized particles (Fig. 4). The simulation shows that the 10 μm particle moves steadily downstream beyond the separation point when the DEP is turned off. This occurs because the velocity of the larger particle (due to the Stokes force) is high enough to move it past the *sp*. After the DEP force is turned on again, the particle has already moved to its next *ep* instead of being pushed back to its original *ep*, causing the particle to undergo a net forward displacement over one cycle. The 3 μm particle, meanwhile, undergoes a zig-zag path over successive on–off cycles. Although the particle does not reach its *sp* during the off period, the DEP force during the on period is too weak to push the particle far back enough. As a result, the small particle is able to move from the present *ep* to the next one over a few cycles of pulsing. For the 5 μm particle, the Stokes and DEP forces are well-matched so that the particle does not attain too high a velocity during the off period and the DEP force is able to push it back to its *ep* during the on period. As a result, the particle exhibits an oscillation motion between *ep* and *sp* in the trap, and it is retained. In this fashion, one can use pulsed DEP to selectively retain intermediate-sized particles.

Separating intermediate-sized particles

To demonstrate the ability to retain intermediate-sized particles from a population with larger and smaller particles, we

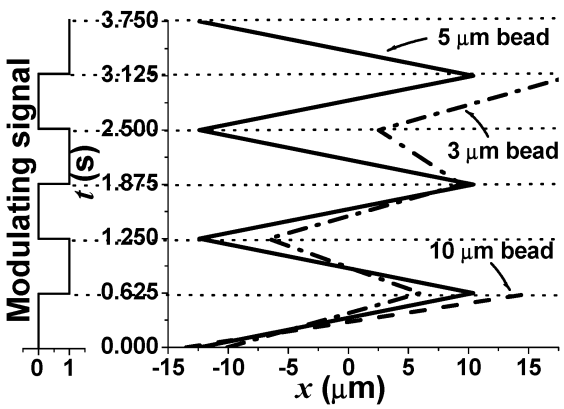

Fig. 4 Simulated particle trajectories in pulsed DEP. Plotted are the trajectories of 3 μm, 5 μm, and 10 μm diameter particles over time at a flowrate of 50 μL/h. The 3 μm and 10 μm particles are released downstream while the 5 μm bead is retained.

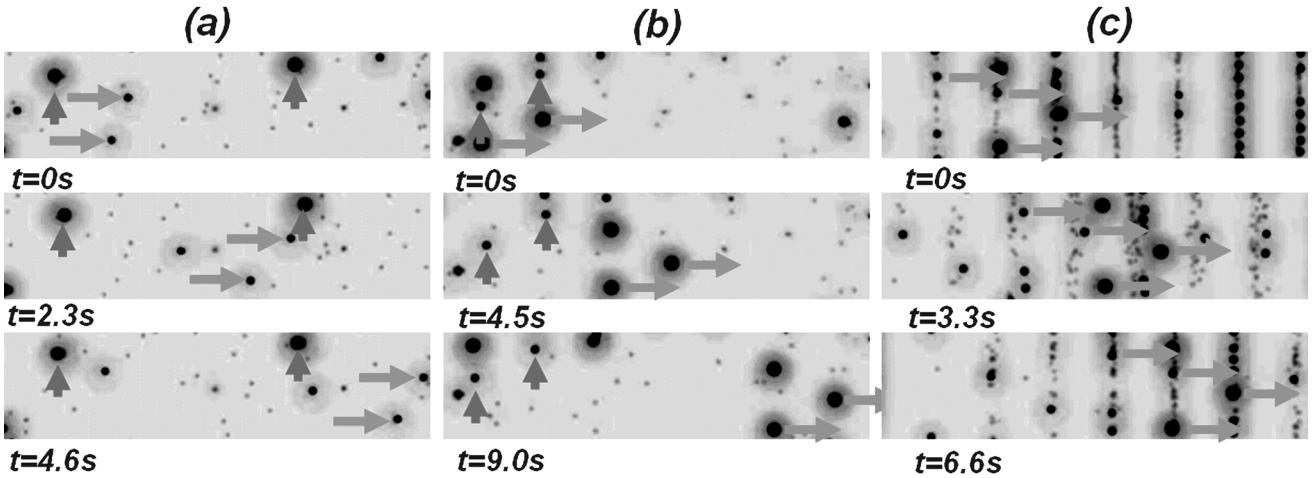

Fig. 5 Retaining different particle sizes. Shown are images of the behaviour of differently sized particles at different pulsing frequencies. (a) At $f = 2$ Hz and $V = 12$ V_{pp}, 10 μm beads are retained while 3 μm and 5 μm beads move downstream. (b) At $f = 1.05$ Hz and $V = 20$ V_{pp}, 5 μm beads are retained, while 3 μm and 10 μm beads move downstream. (c) At $f = 0.3$ Hz and $V = 20$ V_{pp}, 3 μm beads are retained, while both 5 μm and 10 μm beads move downstream. Up arrows (↑) indicate particles that are stopped and right arrows (→) indicate particles that move forward.

performed experiments where we introduced 3 μm, 5 μm, and 10 μm beads into a micro-channel, trapped them using continuous DEP, and then applied pulsed DEP. Results in Fig. 5 depict a time-series of images under different operating conditions (see ESI†).

First, at low voltage (12 V_{pp}), we are below the critical voltage for both the 5 μm and 3 μm particles (Fig. 3b), and thus can only hold the 10 μm particles (Fig. 5a). Over time, the 10 μm beads are retained while 5 μm and 3 μm beads move downstream with the flow. This type of separation is similar to that of a classical size-based separation using continuous DEP.

At higher voltage (20 V_{pp}) but lower pulsing frequency (1.05 Hz), the 5 μm beads are retained, while the larger 10 μm beads and smaller 3 μm beads move downstream with the flow (Fig. 5b), demonstrating that mid-sized particles can be retained using pulsed DEP. Notably, we observed that the 3 μm beads take at least three pulsing cycles to move from one set of electrodes to the next, compared to the 10 μm beads that take only one cycle to move to next electrode. These results are consistent with the predictions in Fig. 4.

Finally, by lowering the pulsing frequency to 0.3 Hz, both 5 μm beads and 10 μm beads move down the channel with the flow in one period, while some of the 3 μm beads drift slowly too. This result is not exactly in agreement with the model prediction. According to the model, the 3 μm beads should be retained for this case. This is probably due to the very weak DEP force set up and Brownian motion effects being significant here. The weak DEP force acting on the 3 μm beads is not able to push the particles to top of the chamber, and Brownian motion effects also keep the particles away from top ceiling. The 3 μm beads will experience a larger Stokes force when it is further away from the top ceiling. Also, the moving 5 μm and 10 μm beads may exert forces and drag the 3 μm beads along, and this effect of neighboring particles is not accounted for in the modeling results for a single bead. Therefore, the behavior of the cluster of beads does not match the model deduced from the individual bead.

Discussion

Pulsed DEP couples a mobility-based separation—as in electrophoresis—with a strength-based separation—as in continuous DEP—by switching the nDEP force on and off. The resulting method is able to size-separate particles in a complementary way to other sized-based separation methods, such as continuous DEP and pinched-flow separation.

Continuous DEP force takes advantage of the cubic dependence of the DEP force on particle radius. In this method, there is a threshold of DEP force needed to retain a particle against flow for a given particle size and electrical properties.[22] Due to the monotonic dependence of the force on particle size, continuous DEP cannot separate out intermediate-sized particles, even when used in conjunction with Stokes drag. The critical distinction is that in continuous DEP, the difference between the applied DEP force and the threshold DEP force does not impact the system dynamics. Pulsed DEP, in contrast, makes use of this difference, embodied in the *ep* and *sp* positions for various size particles.

Pinched-flow fractionation (PFF) is another size-based separation technique where buffer solution pushes particles to the side wall in a pinched-segment of the device to align different size particles.[23] Because of the shear-induced drift near the wall, the separation efficiency depends on the pinched-segment length. Separation is more effective when the pinched-segment is relatively short.[24] Compared to the PFF method, the current method makes use of the vertical component of DEP force to push the particles towards the ceiling of the device. The distance that a particle moves forward when the DEP is turned off is equivalent to the pinched-segment. This length is less than 30 μm in our device and is much shorter than that in the PFF device.

We have been able to develop models and perform experiments to validate the essential features of pulsed-DEP. While the models allow insight into the physics of pulsed DEP, there are discrepancies in the predicted values of voltage *versus* release frequency. For example, the absolute value of the crossing

frequency for 5 and 10 μm beads is higher in experiments (1 Hz) than in the model (0.9 Hz). This discrepancy is likely due to uncertainties in experimental measurements and simplifications in the model. The dipole approximation in the DEP force calculation helps us obtain the analytical expressions. However, this could result in a underestimated DEP force than that by high-order moment method. Additionally, for large particles, the effect of the vertical component of the DEP force, which we neglected in our analysis, becomes more important. For instance, when we ran experiments (not shown) that create a vertical DEP force but no *x*-directed DEP force (using IDEs parallel to the flow direction), we observed that higher voltages (20 V_{pp}) would reduce the particle velocity by about 15% as compared to at low voltage (5 V_{pp}). Thus, the friction between particle and ceiling leads to errors in the model at high voltage.

A relatively low flow rate of 50 μL/h has been used in the experiments reported in this paper, due to limitations in our apparatus to provide a stable flow. If the flow rate is increased, a higher velocity of the particles will require higher electric field and pulsing frequency f_r to be used. Also, any changes to the distance between electrodes will affect the distance between *ep* and *sp*, and the pulsing frequency f_r will have to be adjusted for performing the same sorting operation. Although the experiments have been performed on particles of different sizes, the same principle of sorting, which is based on the relative strength of the Stokes and nDEP force, will also work for particles of different materials. The AC frequency should be chosen in the range where a nDEP force acts on all particles, as determined by their CM factors. The pulsing frequency that should be used to sort the particles in the proper order is determined by the relative strength of the Stokes and nDEP forces, which are dependent on the particle size, electrical properties, flow-rate and voltage applied.

Finally, the design parameters of the device, such as width and spacing between IDEs, height of channel and duty-cycle ratio, could be optimized to improve the separation process for a specific size of particle. More simulation and experimental studies will be performed in the future to determine such optimal design.

Conclusions

We have introduced a dielectrophoresis-based separation method that uses time-pulsing to allow for tunable multiplex separation of particles. Time-pulsing allows separation of particles of different sizes by modulating the time that particles are exposed to DEP forces (on and off) under constant hydrodynamic drag forces. Most importantly, we can tune the operating conditions to elute the small (3 μm), medium (5 μm), or large (10 μm) beads from a mixed population, showing the multiplexing ability of the approach. We developed a model to explain the behavior of particles under pulsed-DEP, and model predictions were consistent with measurements.

Materials and methods

Fabrication of electrodes

The strip electrodes of the device are fabricated from Indium Tin Oxide (ITO) coated glass slides (SPI). These glass slides provide high transparency and good electrical conductivity, enabling visualization of the flow of fluorescent particles in the microchannel. The ITO glass slides were first cleaned by rinsing with isopropanol and acetone three times, blow-dried with compressed nitrogen gas, and then dehydrated on a hot plate at 100 °C for 10 minutes. A positive-tone photoresist AZ2001 is spun-coated at 2500 rpm for 20 seconds with an acceleration of 300 rpm/second, and the slide was baked at 100 °C for 90 seconds prior to standard photolithography. The desired thickness of photoresist is 3 μm. The slide was then exposed to ultraviolet light at about 80 mJ/cm^2 (Karl Suss MA4 Mask Aligner, Waterbury, VT) through a film mask (IGI, Singapore). Subsequently, the slide was immersed into a solution of AZ400K and deionized water (1 : 5) for 20 seconds. The slide is then etched in a solution of ferric chloride (35 g), hydrochloric acid (250 mL) and deionized water (250 mL). The etching time in our experiment is about 2 minutes, after which the slide was immersed in a 5% sodium carbonate solution to remove the surplus etching solution. After the etching process, the slide was rinsed with acetone and water to remove the photoresist, and finally blow-dried.

Fabrication of channels

The sides of the microfluidic channel were made from rectangular SU-8 structures that were patterned on the bottom ITO glass substrate and top glass cover. The bottom rectangle structure was accurately positioned under a mask aligner, while no special treatment was taken for that on the top cover. The dimensions of the top rectangle are a little smaller than the bottom one. The glass cover and ITO glass substrate were placed face to face to form a closed channel, and liquid fast glue is applied to bond the ITO glass and seal the gap between two surfaces. The interlaced side walls of the two rectangular patterns prevent the glue from entering the channel due to capillary force. The actual height of photoresist is obtained by a profiler (Stylus profilermeter, Taylor–Hobson) before bonding. This completes the fabrication of a two-layer chip consisting of the strip electrodes and microfluidic channel.

Fluidics, optics and electronics

Two 1 mm diameter holes were drilled on the ITO glass using a 0.9 mm diamond drill bit mounted on a high-speed drill machine (up to 5000 rpm). A steel needle with 0.8 mm diameter was inserted into the holes, which are then sealed with resin glue to form an interface to the external apparatus outside the microdevice. A 0.5 mm inner-diameter Tygon silicone tube is used to connect the device to a syringe pump. Polystyrene fluorescent microspheres with nominal diameter of about 10 μm, 5 μm and 3 μm were purchased from DUKE Science Corp. The microspheres were mixed with deionized water, and the conductivity of the solution was monitored using a Thermo Electron Russel portable conductivity meter. Finally, the chip was mounted on the stage of an upright microscope (DMLM, Leica) which was supplied with an updating 100 W Hg-lamp. The filters yielded an excitation blue light at 408 nm and an emission green light at about 508 nm. The motion of the fluorescent microspheres was recorded by an image acquiring system. Two

types of signals, continuous and pulsed, were applied to the electrodes to generate the DEP force. Sine-wave signal at 10 MHz with amplitude up to 20 Vpp (with high impedance) was generated by a universal signal generator (Agilent 33220A). The electrical connect was realized through affixing a copper wire to a reserved ITO pad with silver conductive glue.

Testing method

We performed measurements using 3, 5 and 10 μm diameter beads to determine their pulsing frequency related behavior. For the flow rate chosen, flow rate is controlled by syringe pump and several minutes are given for the flow to stabilize in the microchannel. After introducing particles into the chamber, we first turned the voltage to 20 Vpp. Next, we switched the voltage to pulsed mode, and decreased the pulsing frequency gradually from 10 kHz while observing the motion of particles under the microscope. We defined the release frequency as the frequency at which more than 90% of the particles were released at a particular voltage. We then changed to a different voltage and repeated.

Acknowledgements

This work is funded by the Singapore-MIT Alliance under SMA-FRP-2. The authors gratefully acknowledge Dr Wang Zhenfeng, Dr Ng Sum Huan Gary, and Tjeung Ricky Theodore from SIMTech for their kind help with using their microfabrication facilities. The authors also gratefully acknowledge Prof. Lim Siak-Piang, Prof. Khoo Boo-Cheong and Prof. Lee Heow-Pueh for their fruitful discussions.

References

1 D. Pappas and K. Wang, Cellular separations: A review of new challenges in analytical chemistry, *Anal. Chim. Acta*, 2007, **601**, 26–35.
2 P. R. C. Gascoyne and J. Vykoukal, Particle separation by dielectrophoresis, *Electrophoresis*, 2002, **23**(13), 1973–1983.
3 M. P. Hughes, Strategies for dielectrophoretic separation in laboratory-on-a-chip systems, *Electrophoresis*, 2002, **23**(16), 2569–2582.
4 Nicole Pamme, Continuous flow separation in microfluidic devices, *Lab Chip*, 2007, **7**, 1244–1254.
5 H. A. Pohl, *Dielectrophoresis*, Cambridge University Press, Cambridge, UK, 1978.
6 T. B. Jones, *Electromechanics of Particle*, Cambridge University Press, Cambridge, UK, 1995.
7 M. P. Hughes, *Nanoelectromechanics in Engineering and Biology*, CRC Press, Boca Raton, 2003.
8 Joel Voldman, Electrical forces for microscale cell manipulation, *Annu. Rev. Biomed. Eng.*, 2006, **8**, 425–454.
9 Xiao-Bo Wang, Jody Vykoukal, Frederick F. Becker and Peter R. C. Gascoyne, Separation of Polystyrene Microbeads Using Dielectrophoretic Gravitational Field-Flow-Fractionation, *Biophys. J.*, 1998, **74**, 2689–2701.
10 M. D. Vahey and J. Voldman, An equilibrium method for continuous-flow cell sorting using dielectrophoresis, *Anal. Chem*, 2008, **80**(9), 3135–3143.
11 Lisen Wang, Lisa A. Flanagan, Noo Li Jeon, Edwin Monuki and Abraham P. Lee, Dielectrophoresis switching with vertical sidewall electrodes for microfluidic flow cytometry, *Lab Chip*, 2007, **7**, 1114–1120.
12 Ki-Ho Han and A. Bruno Frazier, Lateral-driven continuous dielectrophoretic microseparators for blood cells suspended in a highly conductive medium, *Lab Chip*, 2008, **8**, 1079–1086.
13 R. L. Tornay, T. Braschler, N. Demierre, B. Steitz, A. Finka, H. Hofmann, J. A. Hubbell and P. Renaud, Dielectrophoresis-based particle exchanger for the manipulation and surface functionalization of particles, *Lab Chip*, 2008, **8**, 267–273.
14 Cheng-Ping Luo, Andreas Heeren, Wolfgang Henschel, Monika Fleischer and Dieter P. Kernb, Contactless capturing of particles in liquid using pulsed alternating dielectrophoresis, *J. Vac. Sci. Technol.*, 2006, **24**(6), 3184–3187.
15 J. Regtmeier, R. Eichhorn, T. T. Duong, P. Reimann, D. Anselmetti and A. Ros, Pulsed-field separation of particles in a microfluidic device, *Eur. Phys. J. E*, 2007, **22**(4), 335–340.
16 A. Ajdari and J. Prost, Drift induced by a spatially periodic potential of low symmetry–pulsed dielectrophoresis, *Comptes rendus de l academie des sciences serie II*, 1992, **315**(13), 1635–1639.
17 L. Gorre-Talini, S. Jeanjean and P. Silberzan, Sorting of Brownian particles by the pulsed application of an asymmetric potential, *Phys. Rev. E*, 1997, **56**(2), 2025–2034.
18 Antonio Sarmiento and Hernan Larralde, Deterministic transport in ratchets, *Phys. Rev. E*, 1999, **59**(5), 4878–4883.
19 J. G. Kralj, Michael T. W. Lis, Martin A. Schmidt and Klavs F. Jensen, Continuous Dielectrophoretic Size-Based Particle Sorting, *Anal. Chem.*, 2006, **78**, 5019–5025.
20 Frank M. White, *Fluid mechanics*, Boston, McGraw-Hill, 2003.
21 Michelle E. Staben, Alexander Z. Zinchenko and Robert H. Davis, Motion of a particle between two parallel plane walls in low-Reynolds-number Poiseuille flow, *Phys. Fluids*, 2003, **15**(6), 1711–1733.
22 J. Voldman, R. A. Braff, M. Toner, M. L. Gray and M. A. Schmidt, Holding forces of single-particle dielectrophoretic traps, *Biophys. J.*, 2001, **80**, 531–541.
23 Yamada Masumi, Nakashima Megumi and Seki Minoru, Pinched flow fractionation: Continuous size separation of particles utilizing a laminar flow profile in a pinched microchannel, *Anal. Chem.*, 2004, **76**(18), 5465–5471.
24 Hirosuke Maenaka, Masumi Yamada, Masahiro Yasuda and Minoru Seki, Continuous and size-Dependent sorting of emulsion droplets Using hydrodynamics in pinched microchannels, *Langmuir*, 2008, **24**, 4405–4410.

